Steps towards automatic building of anatomical atlases

Gérard Subsol, Jean-Philippe Thirion, Nicholas Ayache

Epidaure Project, INRIA Sophia-Antipolis
BP 93 - 06 902 - Sophia Antipolis Cedex (France)
e-mail: subsol@epidaure.inria.fr

ABSTRACT

This paper presents a general scheme for the building of anatomical atlases. We propose to use specific and stable features, the crest lines (or ridge lines) which are automatically extracted from 3D images by differential geometry operators. We have developed non-rigid registration technics based on polynomial transformations to find correspondences between lines. We got encouraging results for the building of atlases of the crest lines of the skull and of the brain based on several CT-Scan and MRI images of different patients.

1 INTRODUCTION

In order to improve the diagnosis and therapy planning, the physician needs to compare 3D medical images coming from Computed Tomography, Magnetic Resonance Imagery or Nuclear Medicine.[1] We will not discuss here the problem of multimodality registration but we will still distinguish between three kinds of comparisons: comparison of images of the same patient to study the evolution of a disease, comparison of images of different patients to contrast a healthy and a pathologic person, registration of images with an anatomical atlas.

The aim of anatomical atlas books (for example,[2]) is to compile medical observations and give a qualitative description convenient for a skilled physician. In some cases, they can provide some quantitative information about the localization as the atlas of the brain of Talairach & Tournoux.[3] The next step is to use variability parameters to detect pathologies.

3D medical images provide a tremendous opportunity to improve those atlases and to broaden the scope of their applications. However, medical images can be huge (for instance, a CT-Scan of the skull including $144 \times 512 \times 512$ voxels is 18 Mbytes large); we must therefore develop automatic tools to manage such quantity of data. Furthermore, far better precision can be achieved with 3D image processing technics than with manual ones.

The first attempts to register a 3D image with an electronic atlas are quite old. In 1989, Bajcsy and al.[4] proposed to use an automatic multiresolution elastic deformations process to match a very simplified brain atlas. Marret et al.[5] generalized the concept of deformable Region Of Interest (ROI) templates to construct a tridimensional Volume Of Interest (VOI) brain atlas. In 1991, Greitz et al.[6] developed a precise computerized brain atlas including 11 deformation types. In these two last cases, the matching process remains semi-automatic. We can also notice the head atlas described in[7] which is very detailed but only allows 3D visualization of organs.

0-8194-1698-3/94/$6.00

In this paper, we present our project of an entirely automatic building and use of a quantitative atlas from 3D medical images. Our goal is also to quantify the variabilities of the atlas elements which could lead to automatic diagnosis and surgical planning. After a presentation of the general scheme, we detail the type of features used and also describe precisely a non-rigid registration algorithm. At last, we show some very encouraging results for the automatic building of an atlas of the crest lines extracted from 3D CT-Scan images of skulls and MRI images of brains.

2 GENERAL SCHEME

Our project may be decomposed into two parts (see figure 1):

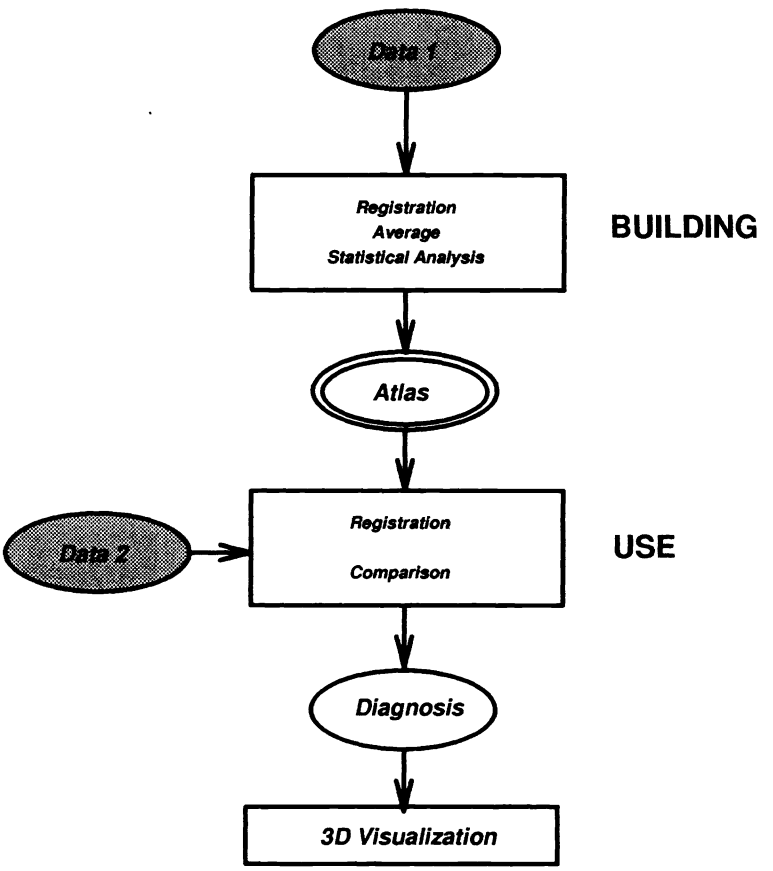

Figure 1: *General scheme*

- *the building*: data 1 is a set of representative objects (for instance, normal patients) which are registered. By making comparisons between the data, the registration algorithm seeks for some features that are shared by the set (or a significant subset). The features "average" will then compose the atlas. A statistical analysis precises the "acceptable difference" in relation to the atlas.
- *the use*: the registration algorithm permits to compare data 2 (for instance, a pathological patient) and the atlas. The statistical parameters give precious information about the level of "abnormality". These results could be sent to a diagnosis module to detect some pathologies. For now, we plan to integrate the

3D visualization of the skull atlas in the craniofacial surgery simulation testbed developed in the Epidaure project[8] in order to help the physician to plan operations.

3 THE ATLAS STRUCTURE

3.1 The features

Raw medical images are stored in a discrete 3D matrix $I = f(x, y, z)$. By thresholding I, isosurfaces of organs are computed (for instance, the surface of the skull for CT-Scan, of the brain or the face for MRI). The problem is then to compute specific features of these surfaces. Several methods have been proposed to achieve this:

- *surface features*: the mean and Gaussian curvatures are used to segment the isosurface into patches of some fundamental types. Such a decomposition permits to study the deformations of the left ventricle[9] or to describe the faces.[10]
- *line features*: Hosaka[11] reports a wide range of characteristic lines based on differential geometry. The 3D Medial Axis Transform gives also sets of lines, charting for instance the gyral anatomy.[12]
- *point features*: the "extremal points",[13] based on geometric invariants are used to perform 3D rigid registration.

A first example of clinical application can be found in Cutting et al.[14] where line and point features are both used to compute "an average" skull. In that study, however, the features are semi-automatically extracted.

3.2 The crest lines

We decided first to use only line features: the crest lines introduced in.[15] They are defined as the successive loci of a surface whose largest principal curvature is locally maximal in the direction of its principal direction (see figure 2). Let k_1 be the principal curvature with maximal curvature in absolute value and $\overrightarrow{t_1}$ the associated principal direction, each point of a crest line verifies: $\overrightarrow{\nabla}\, k_1 . \overrightarrow{t_1} = 0$.

These lines are automatically extracted from an isosurface by the "marching lines" algorithm.[16]

As we can see in the figure 4, crest lines are anatomically meaningful: on the skull, the crest lines represent the salient lines (the orbits, the nose, the mandible or the temples) as emphasized in[17]; on the brain, the crest lines follow the convolutions, the sulci and the giry patterns described in Ono et al..[18]

4 THE REGISTRATION ALGORITHM

4.1 Previous work

The 3D curves registration algorithm is a key point in our scheme: given two sets S and S' composed of the crest lines C_i and C'_j extracted from images of two different patients, we want to find which lines C_i of

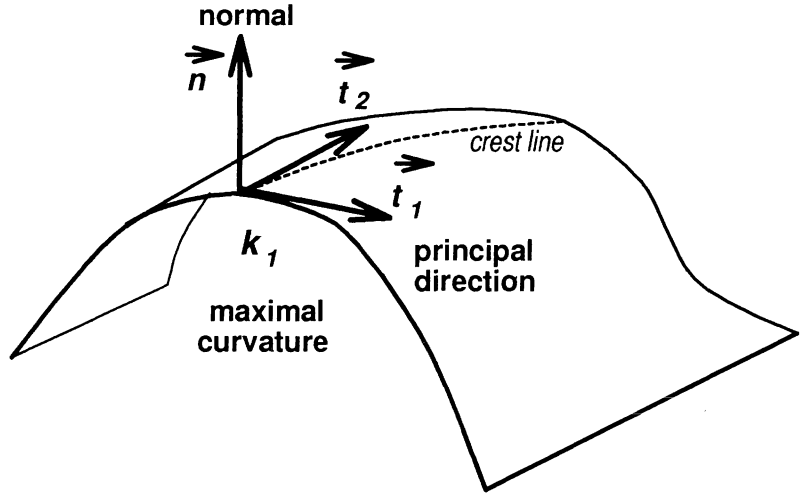

Figure 2: *Differential characteristics of a surface and the crest line.*

S (or portions $P_{i,k}$) correspond to which lines C'_j (or portions $P_{j,l}$) of S' (see figure 3). Two difficulties arise: the number of lines of each set is quite important (several hundreds, sometimes more than a thousand) and the registration between S and S' is not rigid.

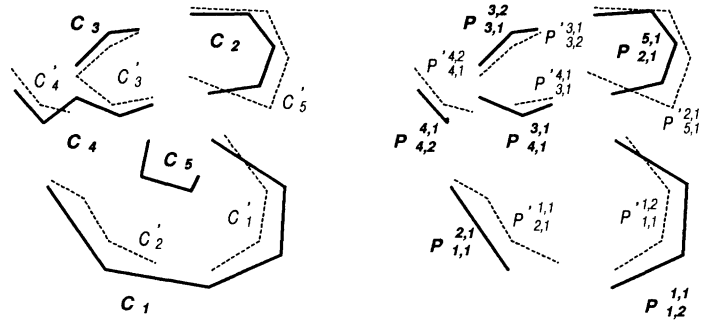

Figure 3: *The registration algorithm has to find the portions $P_{i,k}^{j,l}$ and $P_{j,l}^{'i,k}$, respectively the k^{th} portion of C_i which corresponds to the l^{th} portion of C_j and vice versa.*

In[19] and,[20] 3D curves matching enables to recognize rigid synthetic objects. First, boundary curves are smoothed and then matched with prestored models but the registration is only rigid. In,[21] the algorithm smoothes curves by using non-uniform B-Splines. Then the two sets of curves are matched with an hashing table indexed by euclidean differential invariants. Results are very good[22] especially with sets of crest lines but the method only succeeds in finding a rigid displacement and cannot be generalized easily to the non-rigid case. Zhang in[23] and independently Besl[24] introduced an "iterative closest points" matching method. It consists in three steps: for each point M_i of S, find the closest point M'_i of S'. Then, compute the global rigid displacement between the two sets of matched points $(M_1 \dots M_n)$ and $(M'_1 \dots M'_n)$ by a least-squares technique. Apply this motion to S and iterate until the motion is "small". Both authors use the algorithm to register free-form curves but once again for the rigid case. Nevertheless, we can inprove and generalize this method to our problem.

4.2 The algorithm

Our algorithm follows the steps of the "iterative closest point" method:

- *Points matching*: each point of S is linked with its closest neighbour in S' according to the euclidean distance. We plan also to use in the distance computation the differential curve parameters as the tangent, normal, curvature and torsion[21] or surface parameters as the normal, the principal directions and principal curvatures as described in.[25] We apply some heuristics to make the links symmetrical and consistent along the curves.

  With these couples of points, two coefficients are computed: p_i^j and $p_j^{'i}$ which are the proportion of the curve i of S matched with the curve j of S' and vice versa. Thus, by thresholding, $p_i^j \geq thr$ and $p_j^{'i} \geq thr$, we can determine the curves "registered" at thr percent. For instance, curves can be considered completely registered when $p_i^j \geq 0.5$ and $p_j^{'i} \geq 0.5$.

- *Least-squares transformation*: as the registration is not rigid and even not affine, we try to register S and S' with a 2-order polynomial transformation as in[26] and[27]:

$$\begin{cases} x' = a_1x^2 + a_2y^2 + a_3z^2 + a_4xy + a_5yz + a_6xz + a_7x + a_8y + a_9z + a_{10} \\ y' = b_1x^2 + b_2y^2 + b_3z^2 + b_4xy + b_5yz + b_6xz + b_7x + b_8y + b_9z + b_{10} \\ z' = c_1x^2 + c_2y^2 + c_3z^2 + c_4xy + c_5yz + c_6xz + c_7x + c_8y + c_9z + c_{10} \end{cases}$$

  As these polynomials are linear in their coefficients, we can use the least-squares method,[2829] to compute a_i, b_i and c_i.

  We tried to use higher order polynomials but large unexpected undulations then occur as emphasized in.[30] 2-order polynomial transformations give accurate registration but we are not able to decompose them into intuitive physical meaning transformations such as rotation, translation or scaling. Notice that at each iteration, we compose the transformation with a 2-order polynomial and so, we obtain after n iterations a 2^n-order polynomial transformation.

- *Updating*: the transformation is applied, then the algorithm iterates again or stop according to several criteria (mean value of the distance distribution between matched points, stability of the registration coefficients p_i^j and $p_j^{'i}$, threshold on the matrix norm $||T - I_d||$ where T is the transformation and I_d the identity matrix).

By incrementing the threshold value thr at each iteration, for instance, from 0 to 0.5 by step of 0.025 and by taking only in account the matched point couples (M, M') belonging to "registered" curves at thr percent, the algorithm tends to improve the registration of already matched curves and to discard isolated ones. Moreover, we can begin to apply rigid transformations to align the two sets of lines, then affine tranformations to scale them and, at last, quadratic transformations to refine the registration.

4.3 Results

We applied this algorithm to two sets of the longest crest lines (for easier visualization) of the skulls of two different patients. We can notice in figure 5 (left) that the number of lines of the two sets (42 and 31 lines) and their shape (notice, in particular, the nose) are different and also that the two skulls are quite shifted.

One set of lines S is then deformed to be registered with the second S'. To evaluate the result, we display in figure 5 (right) the registered lines of S' and S after deformation. The matched points are linked by segments.

The registration takes a few minutes on a DEC-Alpha workstation. The algorithm detects and matches similar lines (12 lines) as the orbits, the mandible, the nose, the temples and the occipital foramen.

In figure 6, we show (left) the registered lines of the set S' and of the set S not deformed in order to check the accuracy of the algorithm. We display (right) the deformation applied to a regular mesh. We notice that such a deformation is quite more complex than an affine one.

5 THE ATLAS BUILDING

Given n sets of lines, we can register all the sets two by two. Then, we construct a graph where the nodes are the lines L_i^j where i is the number of the set and j the index of the line in the set S_i and the vertices represent the relation "is registered with". Then, we search for the connected parts of this graph having at least a line of each set. Hence, we have determined the subsets of similar lines that will compose the "atlas".

We have experienced this method with six sets of lines extracted from CT-Scan images of six different dry skulls (figure 7). Notice the difference of size, of shape and orientation. Each set of crest lines is composed from 515 to 544 curves and more than 18000 points. We found 48 subsets of similar lines (figure 8) including the mandible, the nose, the orbits, the cheekbones, the temples, the occipital formaen and the sphenoid and temporal bones. As we labelled some lines of the first skull, we are able to label automatically the subsets and the lines of the other skulls. Notice than the left and right mandible bottom (LMB and RMB) have merged into a unique mandible subset (LMB+RMB).

We also try to obtain the subsets of common lines of three brains automatically segmented from MRI data (figure 9). Each set of crest lines is composed of around 350 curves and 13500 points. In the figure 10, we can distinguish the left and right ventricles and the medulla automatically detected and labelled.

6 FUTURE WORK

Averaging the subsets of line is quite difficult because there is not always a unique line of each set in the subsets and only parts of curves are really registered and have to be taken into account. So, before averaging, we have to find the topology of the common line, i.e. its number of connected parts. Moreover, the curves are sampled independently. So, we will have to construct a consensual coordinate system as emphasized in[14] and, in particular, fix a reference frame.

To compute statistical parameters between the atlas and the data, we are studying the modal decomposition method introduced by Nastar[31] which is well adapted to curves deformations. We can cite also others interesting references as[32] (morphometry applications of shape transformations),[33](decomposition of deformations in principal warps),[34] (Principal Components Analysis on points coordinates) or[35] (shape analysis of the brain based on experimental modes).

This work was partially supported by Digital Equipment Corporation and the Esprit European project Bra-Viva. We thank General-Electric and Bruce Latimer, Director at the Cleveland Museum of Natural History, Court Cutting, David Dean and André Guéziec for the CT-Scan data of the skulls. Jacques Feldmar gave a substantial help in this work.

7 REFERENCES

[1] Nicholas Ayache. Volume Image Processing. Results and Research Challenges. Technical Report 2050, INRIA, September 1993.

[2] Eduard Pernkopf. *Atlas d'anatomie humaine.* Piccin, 1983.

[3] Jean Talairach and Pierre Tournoux. *Co-Planar Stereotaxic Atlas of the Human Brain.* Georg Thieme Verlag, 1988.

[4] Ruzena Bajcsy and Stane Kovačič. Multiresolution Elastic Matching. *Computer Vision, Graphics and Image Processing*, (46):1–21, 1989.

[5] S. Marrett, A. C. Evans, L. Collins, and T. M. Peters. A Volume of Interest (VOI) Atlas for the Analysis of Neurophysiological Image Data. In *Medical Imaging III: Image Processing*, volume 1092, pages 467–477. SPIE, 1989.

[6] Torgny Greitz, Christian Bohm, Sven Holte, and Lars Eriksson. A Computerized Brain Atlas: Construction, Anatomical Content and Some Applications. *Journal of Computer Assisted Tomography*, 15(1):26–38, 1991.

[7] R. Schubert, K. H. Höhne, A. Pommert, M. Riemer, Th. Schiemann, and U. Tiede. Spatial Knowledge Representation for Visualization of Human Anatomy and Function. In H.H. Barrett and A.F. Gmitro, editors, *Information Processing in Medical Imaging*, pages 168–181, Flagstaff, Arizona (USA), June 1993. IPMI'93, Springer-Verlag.

[8] Hervé Delingette, Gérard Subsol, Stéphane Cotin, and Jérôme Pignon. A Craniofacial Surgery Simulation Testbed. In *Visualization in Biomedical Computing '94*, October 1994.

[9] Denis Friboulet, Isabelle E. Magnin, Andreas Pommert, and Michel Amiel. 3D Curvature Features of the Left Ventricle from CT Volumic Images. In *Information Processing in Medical Imaging*, pages 182–192. IPMI'92, 1992.

[10] Vicki Bruce, Anne Coombes, and Robin Richards. Describing the shapes of faces using surface primitives. *Image and Vision Computing*, 11(6):353–363, August 1993.

[11] M. Hosaka. *Modeling of Curves and Surfaces in CAD/CAM.* Springer-Verlag, 1992.

[12] G. Székely, Ch. Brechbühler, O. Kübler, R. Ogniewicz, and T. Budinger. Mapping the human cerebral cortex using 3D medial manifolds. In Richard A. Robb, editor, *Visualization in Biomedical Computing*, pages 130–144, Chapel Hill, North Carolina (USA), October 1992. SPIE.

[13] J.P. Thirion. New feature points based on geometric invariants for 3D image registration. Technical Report 1901, INRIA, May 1993.

[14] Court B. Cutting, Fred L. Bookstein, Betsy Haddad, David Dean, and David Kim. A spline-based approach for averaging three-dimensional curves and surfaces. In David C. Wilson and Wilson Joseph N., editors, *Mathematical Methods in Medical Imaging II 1993*, pages 29–44, San Diego, California (USA), July 1993. SPIE.

[15] Olivier Monga, Serge Benayoun, and Olivier D. Faugeras. Using Partial Derivatives of 3D Images to Extract Typical Surface Features. In *CVPR*, 1992.

[16] J.P. Thirion and A. Gourdon. The Marching Lines Algorithm : new results and proofs. Technical Report 1881, INRIA, March 1993.

[17] Fred L. Bookstein and Court B. Cutting. A proposal for the apprehension of curving cranofacial form in three dimensions. In K. Vig and A. Burdi, editors, *Cranofacial Morphogenesis and Dysmorphogenesis*, pages 127–140. 1988.

[18] Michio Ono, Stefan Kubik, and Chad D. Abernathey. *Atlas of the Cerebral Sulci.* Georg Thieme Verlag, 1990.

[19] C. Marc Bastuscheck, Edith Schonberg, Jacob T. Schwartz, and Micha Sharir. Object recognition by three-dimensional curve matching. *International Journal of Intelligent Systems*, 1:105–132, 1986.

[20] Jacob T. Schwartz and Sharir Micha. Identification of Partially Obscured Objects in Two and Three Dimensions by Matching Noisy Characteristic Curves. *The International Journal of Robotic Research*, 6(2):29–44, Summer 1987.

[21] A. Guéziec and N. Ayache. Smoothing and Matching of 3-D Space Curves. In *Visualization in Biomedical Computing*, pages 259–273, Chapel Hill, North Carolina (USA), October 1992. SPIE.

[22] N. Ayache, A. Guéziec, J.P. Thirion, A. Gourdon, and J. Knoplioch. Evaluating 3D Registration of CT-Scan Images Using Crest Lines. In David C. Wilson and Wilson Joseph N., editors, *Mathematical Methods in Medical Imaging II 1993*, pages 29–44, San Diego, California (USA), July 1993. SPIE.

[23] Zhengyou Zhang. On Local Matching of Free-Form Curves. In David Hogg and Roger Boyle, editors, *British Machine Vision Conference*, pages 347–356, Leeds (United Kingdom), September 1992. British Machine Vision Association, Springer-Verlag.

[24] Paul J. Besl and Neil D. McKay. A Method for Registration of 3-D Shapes. *IEEE PAMI*, 14(2):239–255, February 1992.

[25] Jacques Feldmar and Nicholas Ayache. Rigid and Affine Registration of Smooth Surfaces using Differential Properties. In *ECCV*, Stockholm (Sweden), May 1994. ECCV.

[26] Gerald Q. Maguire, Marilyn E. Noz, Henry Rusinek, Judith Jaeger, Elissa L. Kramer, Joseph J. Sanger, and Gwenn Smith. Graphics Applied to Medical Image Registration. *IEEE Computer Graphics & Applications*, pages 20–27, March 1991.

[27] Ardeshir Goshtasby. Image Registration by Local Approximation Methods. *Image and Vision Computing*, 6(4):255–261, November 1988.

[28] William H. Press, Brian P. Flannery, Saul A. Teukolsky, and William T. Vettening. *Numerical Recipes in C, The Art of Scientific Computing.* Cambridge University Press, 1988.

[29] Å Björck. Algorithms for Linear Least Squares Problems. In Emilio Spedicato, editor, *Computer Algorithms for Solving Linear Algebraic Equations, the State of the Art*, pages 57–92. Springer-Verlag, 1991.

[30] Lisa Gottesfeld Brown. A Survey of Image Registration Techniques. *ACM Computing Surveys*, 24(4):325–376, December 1992.

[31] Chahab Nastar and Nicholas Ayache. Classification of Nonrigid Motion in 3D Images using Physics-Based Vibration Analysis. In *IEEE Workshop on Biomedical Analysis*, pages 61–69, Seattle (USA), June 1994.

[32] Bruno David and Bernard Laurin. Déformations ontogénétiques et évolutives des organismes : l'approche par la méthode des points homologues. *C. R. Académie des Sciences Paris*, II(309):1271–1276, 1989.

[33] Fred L. Bookstein and William D.K. Green. Edge information at landmarks in medical images. In *Visualization in Biomedical Computing 1992*, pages 242–258. SPIE, 1992.

[34] A. Hill, A. Thornham, and C. J. Taylor. Model-Based Interpretation of 3D Medical Images. In Illingworth, John, editor, *British Machine Vision Conference*, volume 2, pages 339–348, Guildford (UK), September 1993. BMVA Press.

[35] John Martin, Alex Pentland, and Ron Kikinis. Shape Analysis of Brain Structures Using Physical and Experimental Modes. In *Applications of Computer Vision in Medical Image Processing*, pages 110–113, Stanford University (USA), March 1994.

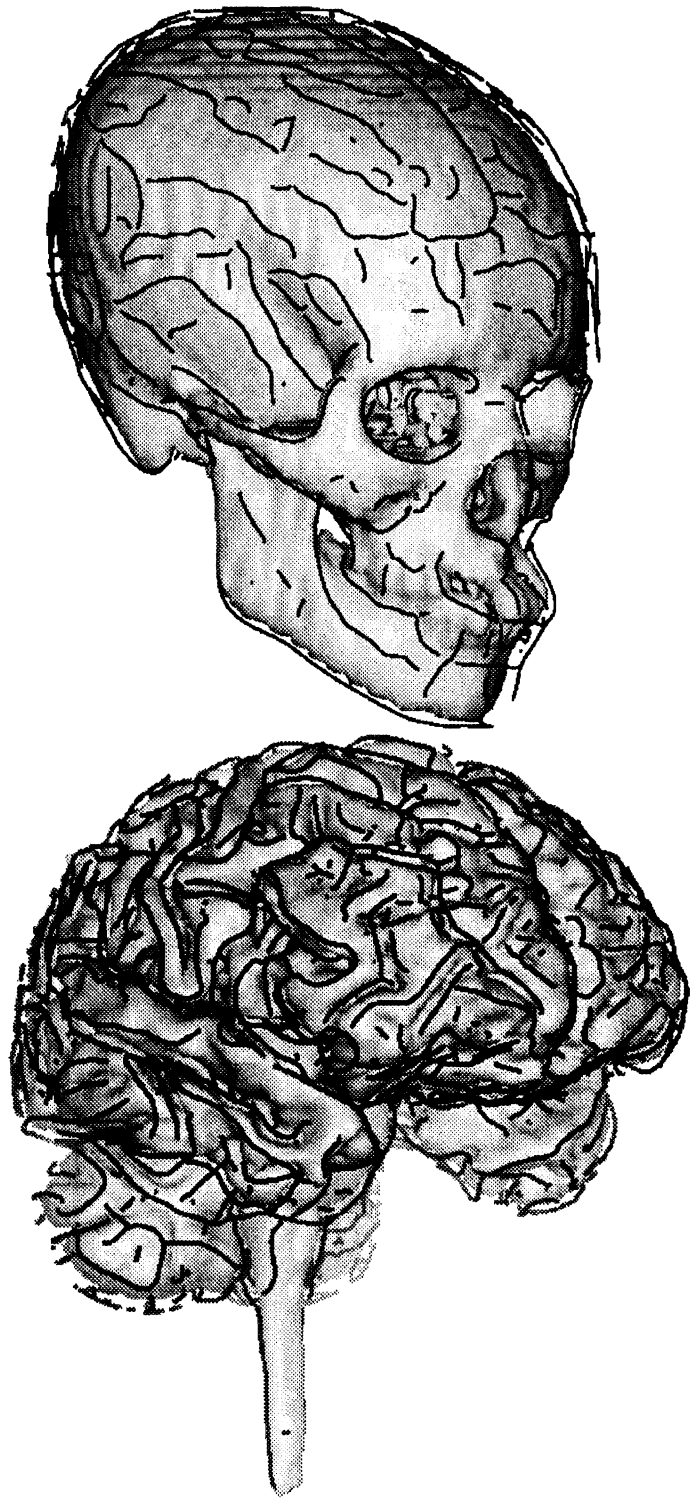

Figure 4: *Crest lines of a skull and of a brain.*

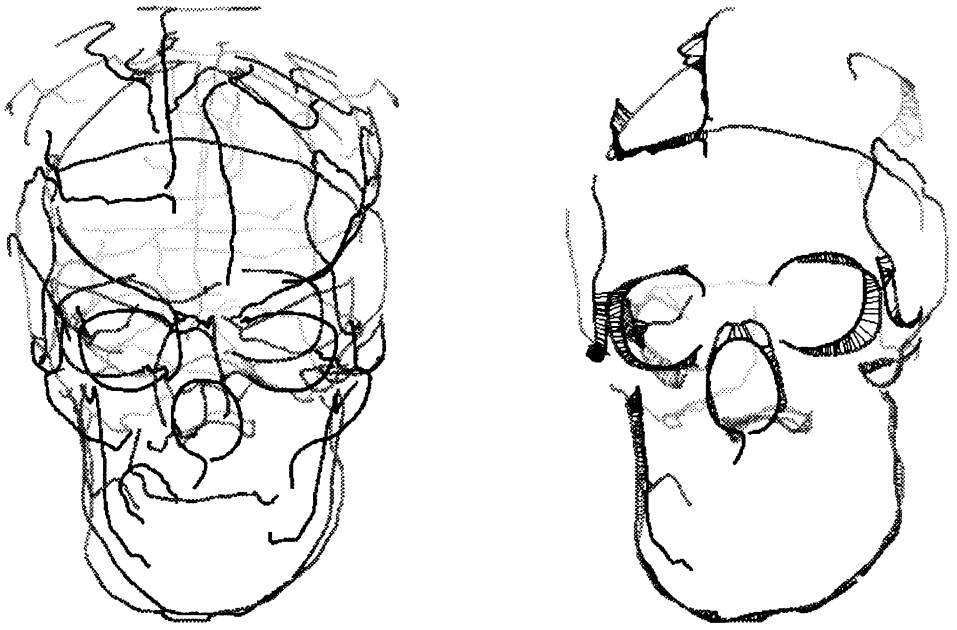

Figure 5: *Left: The longest crest lines of the two skulls superimposed. Right: Registration of similar lines after the deformation.*

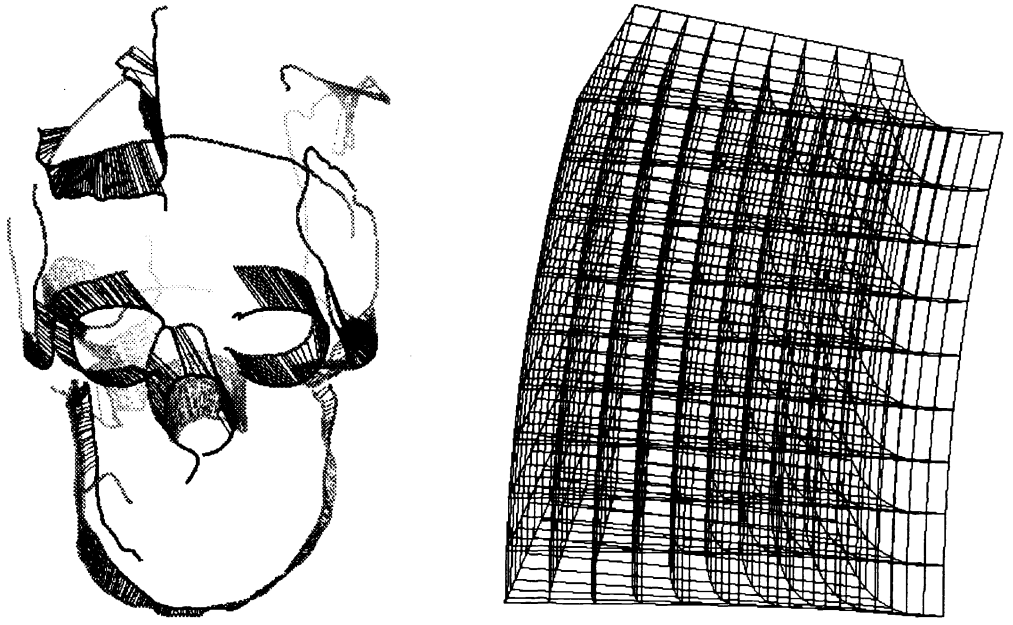

Figure 6: *Left: Registration of similar lines in their original position. Right: The registration deformation applied to a regular mesh.*

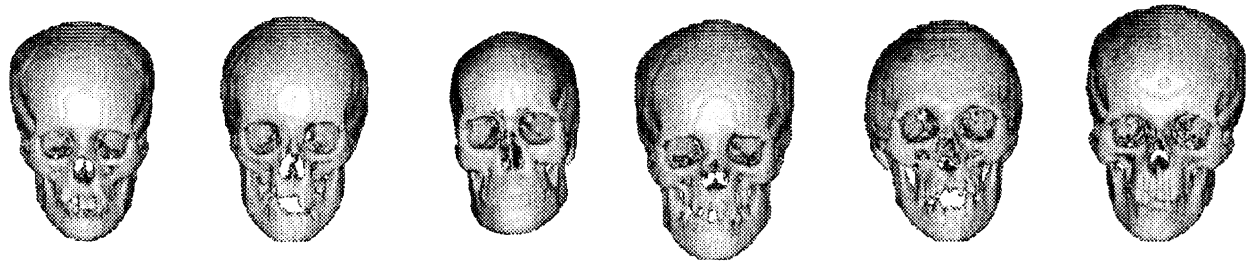

Figure 7: *Six different skulls segmented from CT-Scan data. Notice the difference of shape.*

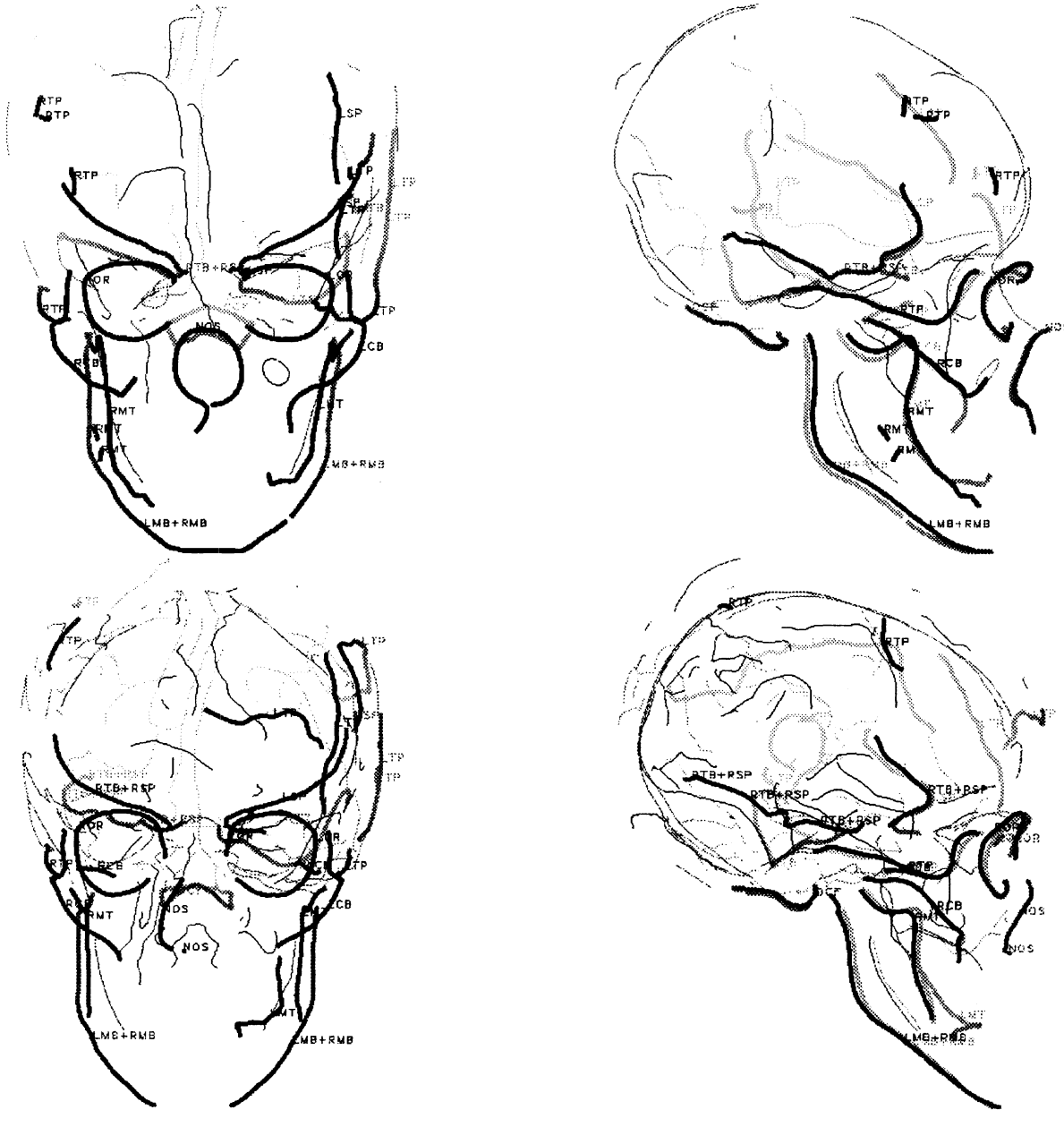

Figure 8: *The structure of the atlas is displayed for the two first skulls. Some subsets of common lines have been automatically labelled and highlighted: the mandible (bottom and up), the nose, the orbits, the cheekbones, the temples, the occipital foramen and the sphenoid and temporal bones.*

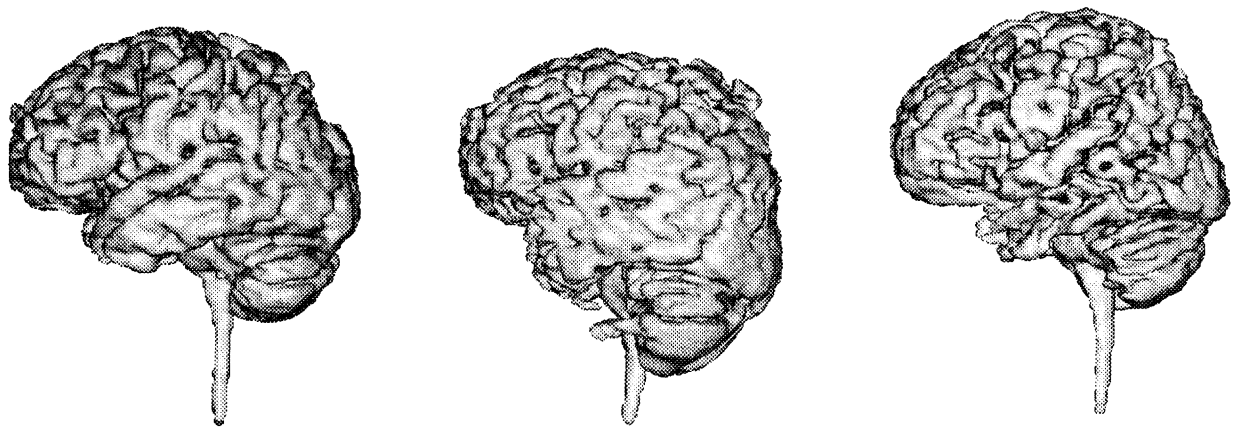

Figure 9: *Three different brains automatically segmented from MRI data of heads. The shape are very different.*

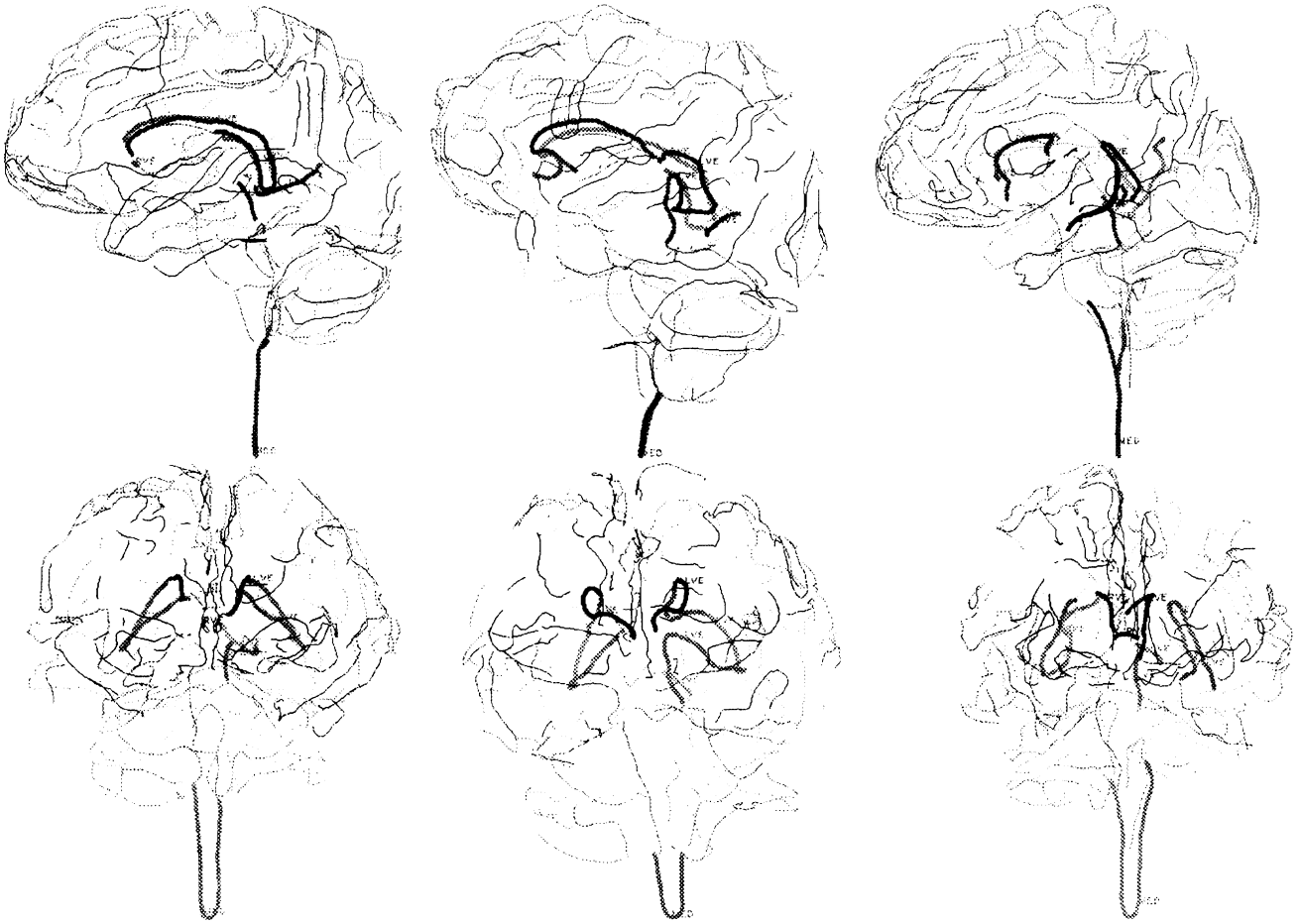

Figure 10: *The structure of the atlas is automatically computed from the three different brains. In particular, the medulla, the left and right ventricles are detected and labelled.*